

# Spectral-Null Pulse Waveform For Characterizing Gain and Phase Distortion in Devices with Uncorrelated Frequency Translation or Limited CW Power Capability

Ralph L. Brooker, *Member, IEEE*

Andrew Corporation, Alexandria, VA 22314, USA

**Abstract** — A test waveform for distortion characterization, denoted Spectral-Null Pulse (SNP), is proposed whose time domain envelope approximates a low duty cycle rectangular pulse, but whose spectrum contains a null at the central spectral line frequency. This spectral line is regenerated by intermodulation distortion in a device under test. The resultant C-I ratio, together with the amplitude compression measured at the pulse peak, may be mapped to AM-PM conversion at the peak amplitude. The technique does not require vector signal analysis and may thus be used to characterize frequency-converting devices with internal oscillators. The technique also permits probing of AM-AM and AM-PM deep into the compression region of high-power devices that cannot tolerate continuous high-level signals.

**Index Terms** — Non-linear distortion, Amplifier distortion, Simulation, Intermodulation distortion, Modeling, Traveling wave tubes.

## I. INTRODUCTION

The problem of relating device transmission distortion parameters such as noise power ratio, adjacent-channel power ratio, and multitone intermodulation is, in general, complex [1]. The task is greatly simplified if the distortion is essentially quasi-static, i.e., there is no memory effect within the signal bandwidth of interest. In this case the device's instantaneous complex transfer function is well predicted by the instantaneous input power and the characteristic gain and phase transfer functions, also known as the AM-AM and AM-PM curves [2], i.e.,

$$20 \log|M_o(t)| = P_o(t) = P_i(t) + G\{P_i\} \quad (1)$$

$$\angle M_o(t) = \angle M_i(t) + \phi\{P_i\} \quad (2)$$

where

$M_o(t)$  = output modulation vector

$M_i(t)$  = the input modulation vector

$P_i(t)$  = instantaneous input power =  $20\log|M_i(t)|$

$G\{P_i\}$  = characteristic nonlinear gain transfer function

$\phi\{P_i\}$  = characteristic nonlinear phase transfer function

Once the transfer functions are established, the nonlinear response may be predicted to any arbitrary input modulation function, such as two-tone or N-tone test signal, NPR waveform, or a communications signal, and the resultant output modulation function may be analyzed for properties such as IP3, NPR, gain compression, or ACPR.

A synchronous vector network analyzer is generally used to measure device transfer curves, but this method is problematic for frequency-converting devices and those that do not tolerate continuous high-level signals. Therefore a characterization technique employing a pulsed stimulus signal and requiring only spectrum magnitude measurement is desirable.

In Fig. 1, example device transfer curves are overlaid by the time-varying amplitude of an ideal pulse stimulus signal that exercises the device under test only at a small-signal power ( $P_{o1}$ ) and at a target large-signal power ( $P_{o2}$ ).

Because the signal dwells only at  $P_{i1}$  and  $P_{i2}$ , the resultant memoryless distortion will be a function only of  $G(P_{i2})$  and  $\phi(P_{i2})$ , and not the behavior between these power points, as would be the case for waveforms such as two-tone or NPR.

If this pulse signal is generated with on-off amplitude keying, the spectrum has lines at all multiples of the pulse repetition frequency (Fig. 2). This is not a useful test signal, however, because the spectrum line magnitudes are only weakly affected by intermodulation distortion.

## II. SPECTRAL NULL PULSE WAVEFORM

In the proposed spectral-null pulse ("SNP") test signal, however, the central spectral line is removed. Moderate distortion in the device under test causes substantial regrowth of this central line due to intermodulation; therefore, C-I (the ratio of the first non-zero tone to the intermodulation product at the center frequency) is sensitive to both amplitude distortion (gain compression/expansion) and phase distortion (AM-PM).

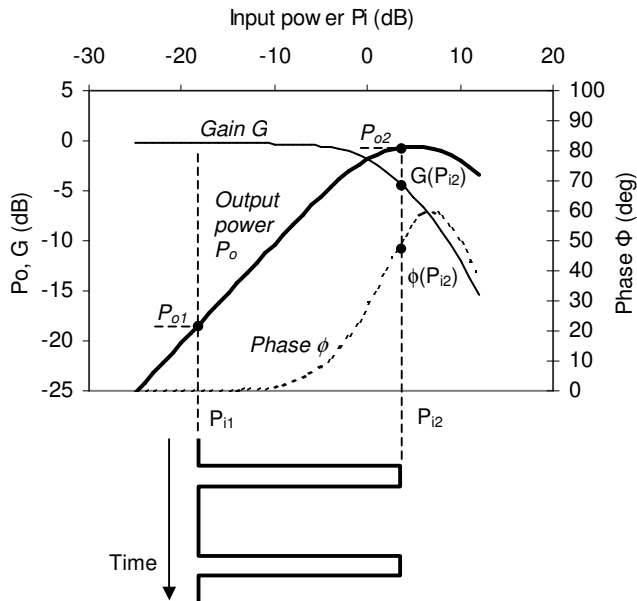


Fig. 1. Typical TWTA nonlinearity exercised by an ideal pulse-envelope waveform. Note that the input envelope has only two amplitude states: (1) small-signal and (2) the large-signal level at which gain and phase are to be measured.

Further, the bandwidth may be confined to the signal bandwidth of interest by applying a Hanning window [3] optimized to trade off between pulse overshoot and rise time. The resultant waveform has spectrum and time-domain magnitudes as shown in Figs. 3 and 4, respectively.

At the output of the device under test, the center carrier will reappear and the peak pulse power will vary from that predicted by small-signal gain alone by the amount of gain compression G<sub>c</sub>, as illustrated in Figs. 5 and 6.

Provided that P<sub>o1</sub> is in the small signal region, gain compression is defined as:

$$G_c = (P_{o2} - P_{i2}) - (P_{o1} - P_{i1}) \quad (3)$$

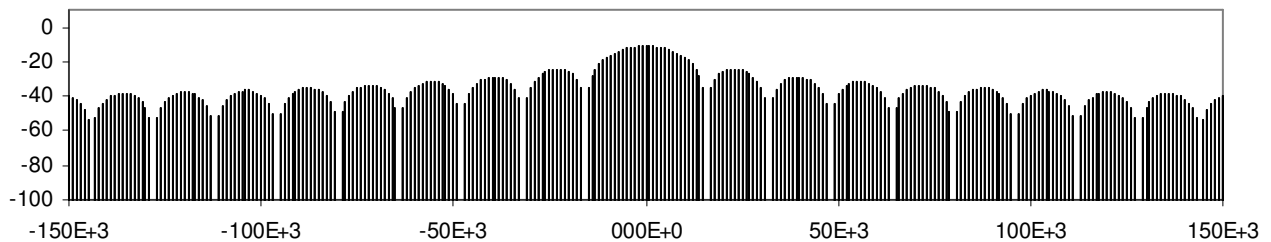


Fig. 2. Spectrum magnitude (dB) vs. frequency offset from carrier (Hz) of an on-off rectangular pulse modulated waveform

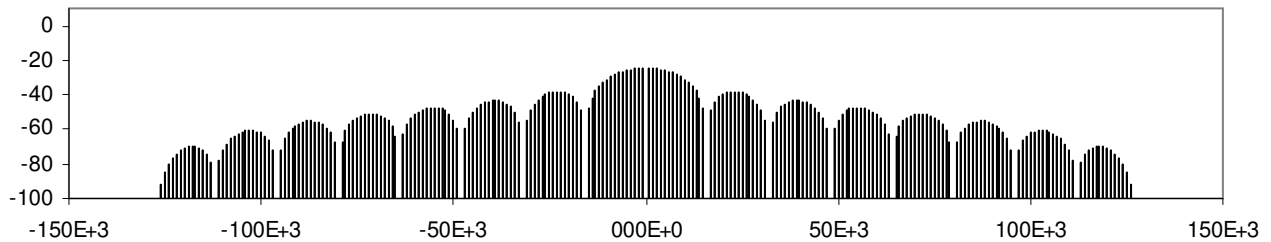


Fig. 3. SNP test signal spectrum magnitude (dB) vs. frequency offset from carrier (Hz). Note the null at center frequency.

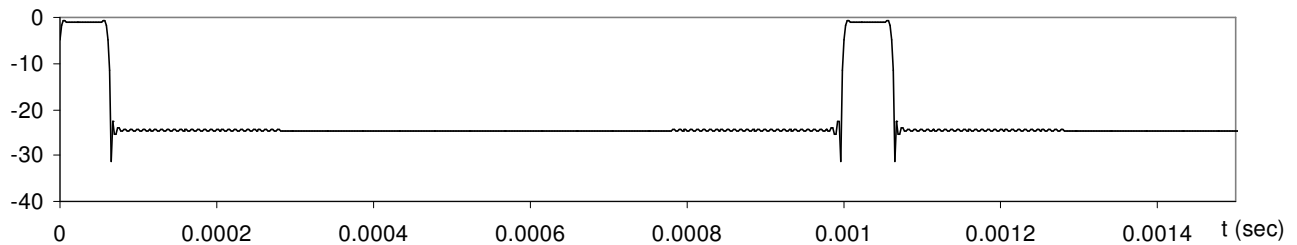


Fig. 4. SNP test signal time-domain magnitude (dB) vs. time.

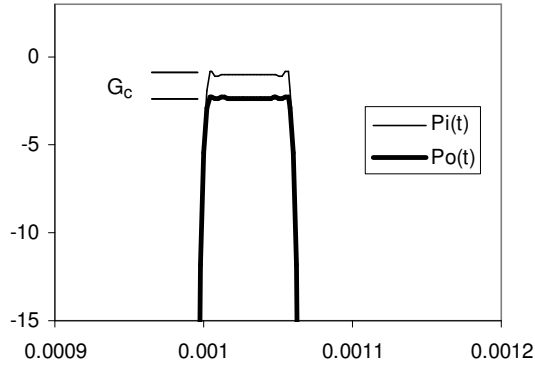


Fig. 5. SNP time domain amplitude detail before and after distortion by a typical TWT at 1.3 dB gain compression. For illustration, the small-signal gain is normalized to zero.

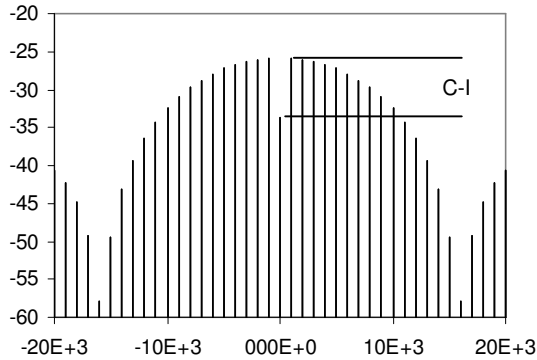


Fig. 6. SNP signal spectrum detail after distortion by a typical TWT at 1.3 dB gain compression. Note regrowth of center carrier.

### III. MAPPING OF C-I TO PHASE

Using envelope simulation, C-I and  $G_c$  may be mapped to  $\phi(P_{i2})$ . If the pulse waveform envelope were perfectly rectangular, the choice of AM-AM and AM-PM transfer curve functions for this simulation would be arbitrary, provided that the gain and phase are both zero at  $P_{i1}$  and that they equal the target gain and phase at  $P_{i2}$ . The envelope has non-zero rise time and some small overshoot, however, owing to the bandwidth restriction of the actual SNP waveform. The transfer curve functions for mapping purposes should therefore be chosen to be well behaved in the power range between  $P_{i1}$  and  $P_{i2}$ . A simple straight-line (dB) function pair is a reasonable starting point:

$$\begin{aligned} G(P_i)_{\text{dB}} &= 0 && \text{for } P_i < 0 \\ &= (P_i/P_{i2}) \cdot G_T && \text{for } P_i \geq 0 \end{aligned} \quad (4)$$

$$\begin{aligned} \phi(P_i) &= 0 && \text{for } P_i < 0 \\ &= (P_i/P_{i2}) \cdot \phi_T && \text{for } P_i \geq 0 \end{aligned} \quad (5)$$

where  $G_T$  is the gain target at  $P_{i2}$ ,  $\phi_T$  is the phase shift target at  $P_{i2}$ , and  $P_{i2}$  is the SNP peak pulse power.  $P_{i2}$  is chosen such that the  $P_{i1}$  of the waveform is approximately  $-P_{i2}$ , i.e., the waveform is generally centered on  $P_i = 0$  dB.

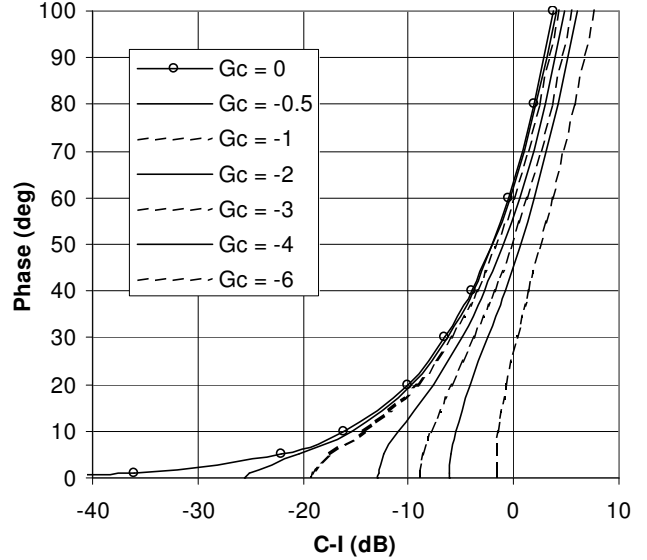


Fig. 7. Mapping function of phase  $\phi$  (AM-PM) vs. C-I and  $G_c < 0$  (gain compression)

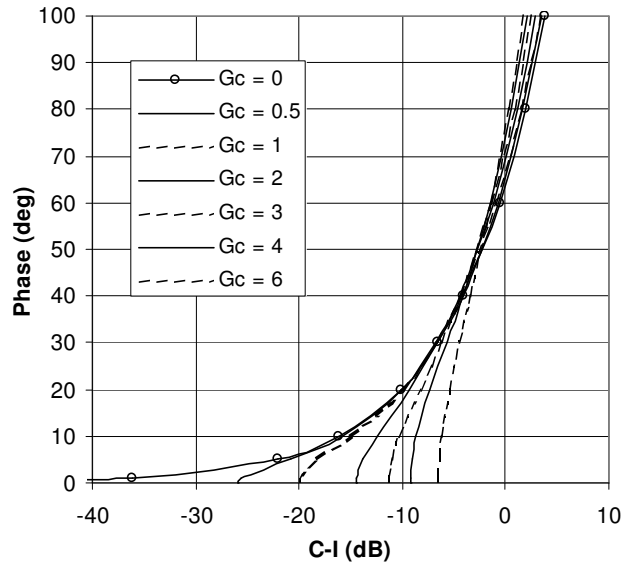


Fig. 8. Mapping function of phase  $\phi$  (AM-PM) vs. C-I and  $G_c > 0$  (gain expansion)

Example mappings using this method for an SNP waveform with 6.25% duty cycle are shown in Fig. 7 for  $G_c < 0$  (gain compression) and Fig. 8 for  $G_c > 0$  (gain expansion).

The simulation was made in Microsoft Excel using macro code written in Visual Basic for Applications. The algorithm uses the method of point-by-point time-domain mapping of input to output gain and phase according to the transfer curves, followed by an FFT to determine C-I.

#### IV. GENERATION OF THE SNP WAVEFORM

The algorithm for generating the complex envelope of the SNP waveform is as follows.

##### 1. Choose waveform parameters:

$f_s$  = spectral line spacing = pulse repetition rate;

$k$  = duty cycle ratio

Note: on-off power ratio =  $20 \log(k)$  and peak-to-average power ratio =  $10 \log[k(1+k^{-2})]$

$n_t$  = number of tones;

$f_w$  = the Hanning window width ratio;

$t_s$  = sampling interval.

##### 2. Generate the Hanning/null filter linear transfer function $H(f)$ , where $\text{ang}[H(f)] = 0$ , and $|H(f)|$ is according to Table 1, where

$$f_{\max} = 1/(2 t_s)$$

$$f_c = (n_t / 2)(f_s / f_{\max}) - f_w$$

TABLE I  
HANNING/NUL MAGNITUDE FUNCTION

$f$	$ H(f) $
$f = 0$ (center null)	0
$f > 0$ to $ f /f_{\max} < f_c - f_w$	1
$ f /f_{\max} \geq f_c - f_w$ to $ f /f_{\max} < f_c + f_w$	$\{1/2 [1 - \sin(\pi ( f /f_{\max} - f_c) / 2 f_w)]\}^{1/2}$
$ f /f_{\max} \geq f_c + f_w$	0

##### 3. Generate the SNP complex envelope spectrum

$$S_{\text{SNP}}(f) = H(f) \cdot S_p(f)$$

where  $S_p(f)$  is the complex spectrum of the rectangular pulse waveform with duty cycle  $k$ .

##### 4. Optionally, offset the spectrum by $f_s/2$ , in order to shift the desired IMD product away from any generator DC leakage term, as described below.

##### 5. Generate the time-domain I and Q sequences by taking the inverse Fourier transform.

Example: The waveforms and spectra in Figs. 3 and 4 were created with  $f_s = 1$  kHz,  $k = 6.25\%$ ,  $n_t = 256$ ;  $f_w = 0.25$ ,  $t_s = 1.953$  ms. This signal has a duty cycle of 6.25%, an on-off ratio of 24.1 dB, and a peak-to-average power ratio (PAPR) of 11.8 dB.

#### V. PRACTICAL CONSIDERATIONS

##### A. Measurement Configuration

An example measurement configuration is shown in Fig. 9. The control computer generates the I and Q envelope waveforms and downloads them to the vector signal generator. The spectrum analyzer is operated in zero-span, wide-bandwidth mode to measure  $P_{O2}$  from the time domain waveform; it is then operated in swept narrow-bandwidth mode to measure C-I. To build the complete characterization table,  $P_{i1}$  and  $P_{i2}$  are stepped together. In the Agilent E4438C signal generator, overall input power may be adjusted without affecting the SNP modulation waveform. At each point, C-I and  $P_{O2}$  are measured and mapped to large-signal gain and phase.

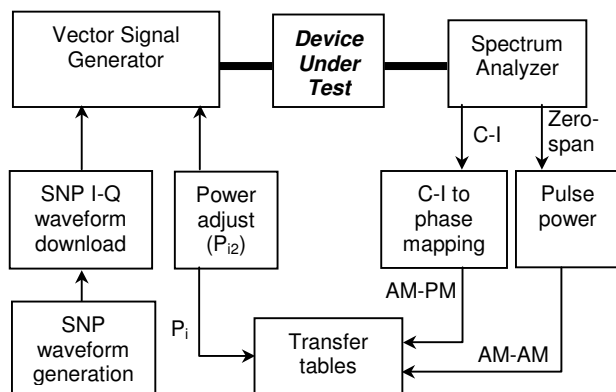


Fig. 9. Measurement equipment configuration and processing flow.

##### B. Calibration

The spectrum analyzer absolute power reading is calibrated against a power meter with the analyzer in zero-span mode using a low-level CW signal.

### C. Residual DC term

Imperfect modulator quadrature balance in the vector signal generator may cause a zero-frequency term to appear at levels large enough to obscure the intermodulation product generated in the device under test. In generators such as the Agilent E4438C, I-Q gain balance and phase skew may be manually adjusted to achieve a center-frequency null. Further, the entire SNP spectrum may be offset by  $f_s/2$ . This shifts the desired distortion product away from the generator's DC term, making it readily measurable to low levels.

### D. Phase ambiguity

The C-I value for any pair of transfer functions  $G(P_i)$  and  $\phi(P_i)$  will be identical if the phase response is replaced with  $-\phi(P_i)$ . Therefore it is not possible to determine the sign of the phase transfer function from C-I alone. Often, however, the sign is known *a priori*; for example, in TWT amplifiers phase shift is negative.

## VI. APPLICATIONS

The SNP technique is most useful when continuous-signal vector network analyzers cannot be used.

### A. Frequency-Converting Devices

In frequency converting devices with inaccessible local oscillators, vector network analysis cannot normally be used. Even if the LO can be frequency locked to an external reference (for example, in a satellite block upconverter) it will generally not be phase coherent with a translating vector network analyzer, even if both are locked to the same external frequency reference. The SNP technique overcomes this restriction by requiring only scalar spectrum analysis.

### B. Devices Intolerant of High Continuous Power

The maximum continuous output power of high peak-power amplifiers is often restricted by thermal dissipation. By setting the pulse duration to be shorter than the device's thermal time constant and setting the duty cycle low enough to maintain average power within safe limits, the SNP technique allows compression and AM-PM to be characterized into the saturation region without damage to the amplifier. This capability enables prediction of multi-carrier intermodulation or NPR performance when the aggregate average signal level is near the CW rated power, because the peak signal powers in the application reach the same levels of the device's operating region that are exercised by the SNP characterization waveform.

### C. Broadband Devices

The SNP technique is useful for distortion characterization of very wide bandwidth systems for which in-band IMD is of greater importance than spectral spreading. This situation might occur, for example, when the signal occupies its full bandwidth allocation and any out-of-band IMD is removed by filtering. Other wideband characterization methods may not indicate in-band distortion characteristics as well.

## VII. VALIDATION OF THE MEMORYLESS ASSUMPTION

Memory effect, up to the modulation bandwidth of the generator, can be detected by varying the repetition rate  $f_s$ . (In the E4438C generator,  $f_s$  may be varied without affecting the I-Q waveform.) If a memory effect is present, C-I will vary with  $f_s$ . Temporal manifestations of memory effects will be visible as pulse shape distortion.

## VIII. CONCLUSION

The SNP waveform permits characterization of envelope gain and phase distortion using only scalar spectrum analysis. It provides a more direct mapping of intermodulation product levels to AM-AM and AM-PM distortion than conventional multitone or NPR techniques. It is particularly useful for characterizing devices that cannot be measured with a continuous signal or whose input and output signals are not phase coherent.

## ACKNOWLEDGEMENTS

The author thanks Pat McHale and Erland Hval of Agilent Technologies for their assistance with E4438C configuration and waveform programming.

## REFERENCES

- [1] Jose Carlos Pedro and Nuno Borges de Carvalho, "On the Use of Multitone Techniques for Assessing RF Components' Intermodulation Distortion," *IEEE Trans. Microwave Theory & Tech.*, Vol. 47, pp. 2393-2402, December 1999.
- [2] A. Saleh, "Frequency-independent and frequency-dependent models for TWT amplifiers," *IEEE Trans. Communications*, COM-29, pp.1715-1720, November 1981.
- [3] M. E. Van Valkenburg (Ed.) and W. E. Middleton (Ed.), *Reference Data for Engineers: Radio, Electronics, Computer, and Communications*, Boston: Newnes, 2002.